Corrosion Inhibition on Mild Steel using Zinc Phosphating Modified with Magnesium and Calcium Additives

Ayoola A. A.[1, *], Durodola M. B.[2], Babalola R.[3], Fayomi O. S. I.[4], Okoji A.[1], Agbeyegbe G. A.[1] and Obigwe C.[1]

[1]*Chemical Engineering Department, Covenant University, Ogun State, Nigeria*
[2]*Chemistry Department, Covenant University, Ogun State, Nigeria*
[3]*Chemical/Petrochemical Engineering Department, Akwa Ibom State University, Nigeria*
[4]*Mechanical and Biomedical Engineering Department, Bells University of Technology, Ota, Ogun State, Nigeria*
[*]Corresponding author: ayodeji.ayoola@covenantuniversity.edu.ng

Received 03/02/2024; accepted 25/06/2024
https://doi.org/10.4152/pea.2026440201

Abstract
MS is a very versatile and useful alloy in metal industry, since it is available and affordable, but it is prone to corrosion. This study investigated MS corrosion inhibition by modifying $Zn_3(PO_4)_2$ bath with MgO and, then, with combined MgO and CaO additives. Different phosphating times (40, 60 and 80 min) and T (65 and 80 °C) were considered. Ct from 0 to 1.8 g/L MgO and combined MgO/CaO additives were added to $Zn_3(PO_4)_2$ bath. SEM analysis of the coated samples was carried out. The specimens were also immersed in 3.5 wt% NaCl, for WL testing. Obtained results showed that the highest IE(%) of 56% was obtained for the MS sample at a phosphating T of 65 °C and Ct of 1.8 g/L MgO additive. For combined MgO and CaO additive, an IE(%) of 32% was obtained, at 65 °C, with a Ct of 0.9 g/L. MgO and CaO adsorption process (separately and combined) onto MS followed Freundlich's adsorption model. ΔG indicated a physical adsorption process, and ΔH indicated an exothermic adsorption process, while ΔS during coating revealed a decrease in the process randomness degree.

Keywords: Ca additive; corrosion; Mg additive; MS; Zn phosphating.

Introduction•

Corrosion is the gradual degradation and loss of metallic materials' main properties, due to chemical reactions between their exposed surface and acidic media of an electrochemical system [1].

This electrochemical phenomenon is caused by the presence of anodic and cathodic sites on metals surface, resulting from the heterogeneous behaviour of the material's surface and bulk [2, 3].

Corrosion has many and varied consequences on the reliability, efficiency, and safety of buildings, metallic equipment or machinery. These effects are frequently worse than the simple loss of metal structures. The varied degree of loss, failure or damage can cause millions of dollars or loss of lives and properties [4-7].

Phosphating is a preferred corrosion prevention method for metal surface treatment and finishing, which comprises the formation of a fine coating on both ferrous and non-

•The abbreviations and symbols definition lists are in page 93.

ferrous metals. It is widely used in automobile, power and aviation industries. This method is highly regarded for its efficiency, rapid operation and ability to provide outstanding corrosion and wear resistance, adhesion, and lubricative properties [8, 9].
Initially, the process was developed as an easy way to prevent corrosion, but as the end uses for phosphated products have changed, it has become necessary to modify current procedures and develop new methods to replace conventional ones [9, 10].
Conventional PB consist of diluted solutions based on H_3PO_4, which incorporate one or more alkali metal or heavy metal ions. These baths predominantly contain primary PO_4^{3-} of metal ions and free H_3PO_4 (Eq. 1).

$$\text{Fe}+2H_3PO_4 \rightarrow Fe(H_2PO_4)_2 + H_2 \uparrow \quad (1)$$

This reaction occurs when a MS panel (to be phosphated) is added to a PB solution, and free H_3PO_4 in the bath starts Fe dissolution at the microanodes contained on the substrate. At micro cathodic sites, hydrogen evolution takes place [11, 12].
$Zn_3(PO_4)_2$, which involves the introduction of Zn into the PB stands out as a promising technique to enhance Fe and steel corrosion resistance. The addition of certain metal salts to PB has been found to exert a notable influence on the microstructure of PC, resulting in denser and finer coatings [9].
$Zn_3(PO_4)_2$ is an inorganic compound. The two common potential outcomes of $Zn_3(PO_4)_2$ bath reaction are shown in Eqs. 2 and 3 [13].

$$3Zn^{2+} + 2H_2PO_4^- + 4H_2O \rightarrow Zn_3(PO_4)_2.4H_2O + 4H^+ \quad (2)$$

$$Zn^{2+} + Fe^{2+} + 2H_2PO_4^- + 4H_2O \rightarrow Zn_2Fe(PO_4)_2.4H_2O + 4H^+ \quad (3)$$

Increased corrosion resistance and surface preparation for painting are two common applications of $Zn_3(PO_4)_2$ conversion coatings. For reinforced concrete, this form of treatment has just recently been developed. There has been ongoing development and modification of $Zn_3(PO_4)_2$ solutions to improve coating properties, including alkaline stability and corrosion resistance [14, 15].
To enhance PC qualities, many additive types are employed in PB. This research focused on how these additives affected PC's effectiveness. Metal cations like Ni^{2+}, Ca^{2+}, Mn^{2+}, Mg^{2+}, Cu^{2+} and Mo^{2+} were among the investigated additives. The results of the variation in formulation parameters of a PB containing varying Ct of corrosion controlling CaO and MgO additives (separate and combined), with a $Zn_3(PO_4)_2$ bath, at two different T of 65 and 80 ºC, and different times (40-80 min) were examined.

Materials and methods

Pre-treatment of MS

MS chemical compositions was analysed using XRF spectrometer (TEFA ORTEC, USA). Each MS sample had the dimensions of 25 x 25 cm, with a tiny hole at the edge region, to ensure the suspension of the sample in the PB solution. The MS surfaces were polished using emery papers of different size ranges. A 0.2 M sodium hydroxide solution was first used for degreasing the MS surface. Then, the samples were rinsed in distilled water. The MS specimens were suspended in a 0.2 M hydrogen chloride solution, and rinsed in distilled water, for 2 min. Then, the surface activation was achieved by dipping each sample in a hydrogen peroxide solution and, then, distilled water.

PB

PB's components used is as shown in Table 1. All reagents were of analytical grade.

Table 1: Components of PB.

Constituent	Value
ZnO (99%, Fischer Chemical)	5 g/L
$NaNO_2$ (97%, Molychem)	0.1 g/L
$ZnNO_3$ (96%, Qualikems)	0.2 g/L
MgO and CaO additives (Molychem)	0, 0.9 and 1.8 g/L
H_3PO_4 (99%, Sigma Aldrich)	30 mL

Design of experiment

Experimental design adopted for the PC process is shown in Table 2.

Table 2: Design of experiment for $C_0C_1C_3$ process.

T (ºC)	Time (min)		
65	40	40	40
	60	60	60
	80	80	80
80	40	40	40
	60	60	60
	80	80	80

The experiments were carried out at two different T of 65 and 80 ºC. At each T, three different coating times (40, 60 and 80 min) and Ct (0, 0.9 and 1.8 g/L) of additives were considered. MgO and combined MgO and CaO (50-50) additives were used during the phosphating process. Hence, a total of 54 experimental runs were carried out.

WL analysis of the coated sample

For the corrosion test, coated samples were immersed in a 3.5 wt% NaCl solution, during 10 days. The WL of each sample was evaluated at every 48 h (2 days).

Analysis of coated samples

The surface structures of the coated samples were analysed using SEM analysis (Jeol SEM, Jeol JSM – 7600F UHR Analytical FEG SEM).

Adsorption isotherm of the PC mechanism

The adsorption mechanism of the PC process was established by considering both Langmuir's and Freundlich's isotherms. Langmuir's and Freundlich's adsorption isotherms are expressed in Eqs. (4) and (5), respectively.

$$\frac{C_{ads}}{\theta} = \frac{1}{K_{ads}} + C_{ads} \quad (4)$$

$$\log \theta = \log K_{ads} + \frac{1}{n} \log C_{ads} \quad (5)$$

where C_{ads} = Ct of adsorbate adsorption onto the MS surface. A plot of $\log \theta$ against $\log C_{ads}$ gives a slope of $\frac{1}{n}$ and an intercept of $\log K_{ads}$.

Thermodynamics of the adsorption process

To further analyse the adsorption mechanism, thermodynamic parameters (such as ΔS, ΔG and ΔH of the PC adsorption process) were evaluated using Eqs. (6-8).

$$\Delta G = -RT \ln K \quad (6)$$

$$\Delta G = \Delta H - T\Delta S \quad (7)$$

$$\ln K = \frac{\Delta S}{R} - \frac{\Delta H}{RT} \quad (8)$$

where R = gas constant (8.314 J/mol/k) and K = thermodynamics equilibrium constant of the adsorption process.

Results and discussion

XRF results for MS

XRF results for MS are shown in Table 3.

Table 3: Elemental compositions of MS sample.

Elements	Composition (%)
Fe	88.10
Al	0.14
Mn	0.30
Ca	0.80
P	0.01
K	0.02
Mg	0.50
Sn	4.67
Cu	4.70

The results revealed Fe (88.1%) as the main element of te MS. That is, the sample used in experimental work was Fe based, as reported in literature [16].

SEM of phosphating samples

SEM results for uncoated and coated MS samples, at 65 °C, and 0.9 and 1.8 g/L Ct of Mg additive, are shown in Fig. 1(i–vi), with 8000X magnification.

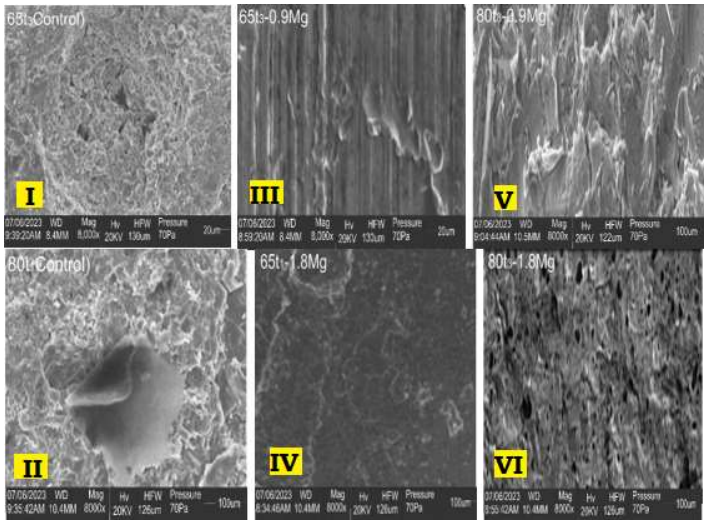

Figure 1: (i-vi) SEM of phosphated MS samples (with Mg additive).

Generally, the two samples without Mg additive (Fig. 1(i–ii)) appeared to be worse coated than the other four specimens. These results revealed that Mg added to the PB solution is as an agent that promotes fine particles distribution on the MS samples surface.

At 65 ℃ phosphating T, the sample with 1.8 g/L Mg (Fig. 1(iv)) was better coated than the sample with 0.9 g/L Mg (Fig. 1(iii)). This showed that the Ct of Mg influenced the PC surface morphology (texture and distribution) on the MS surface. That is, higher Ct of Mg additive promoted smoother coating deposition.

At 80 ℃ phosphating T (Fig. 1(v-vi)), better particles distribution was observed with 0.9 g/L Ct of Mg additive than that with 1.8 g/L. This indicated that T above 65 ℃ did not support increased Mg additive Ct beyond 0.9 g/L. This result confirmed that, as commonly reported in literature, 65 ℃ is the optimal phosphating T for MS [12].

Fig. 2(i-iv) shows the SEM analysis of the phosphated samples (with combined Ca and Mg additives) at two different T and Ct. In general, a perfect and orderly distribution of particles on the MS surface was seen with 0.9 g/L combined additives, at 65 ℃, compared to any other phosphating conditions. From Fig. 2(i-ii), it could be deduced that the lower 0.9 g/L Ct of combined Ca and Mg additives favoured better grain particles distribution than the 1.8 g/L Ct. At 80 ℃ phosphating T, a stronger coating was observed with 1.8 g/L Ct of the combined additives. That is, decreased T favoured lower Ct of the combined additives. Thus, higher phosphating T favoured higher Ct of the combined additives. Hence, the synergetic performance of Ca and Mg additives was achieved either at decreased T (65 ℃) and lower Ct (0.9 g/L) or at increased T (80 ℃) and higher Ct (1.8 g/L).

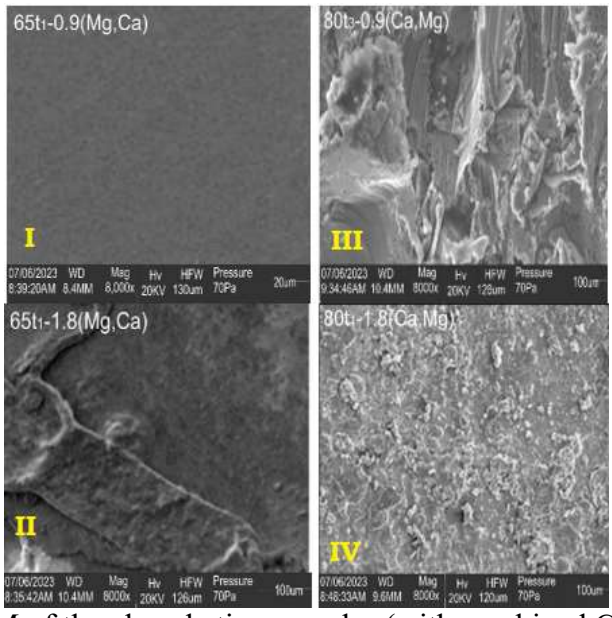

Figure 2: (i-iv) SEM of the phosphating samples (with combined Ca and Mg additive).

PC weight

Fig. 3(i–ii) shows the results of both the PC weight of the samples. The results obtained from the SEM analysis were corroborated by the results obtained from the PC weights of the coated samples.

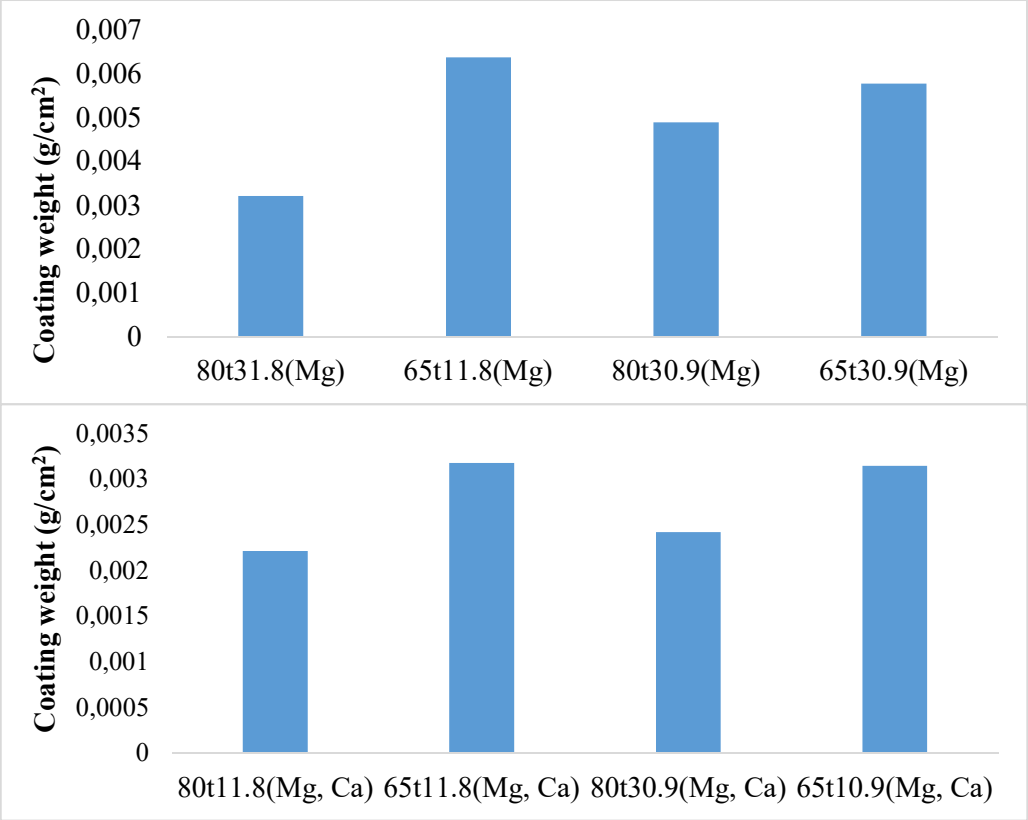

Figure 3: (i-ii) PC weight of samples with MgO and with MgO + CaO added to the PC bath.

CR of the samples

Fig. 4 shows CR results for both coated and uncoated MS samples (with indicated PC conditions).

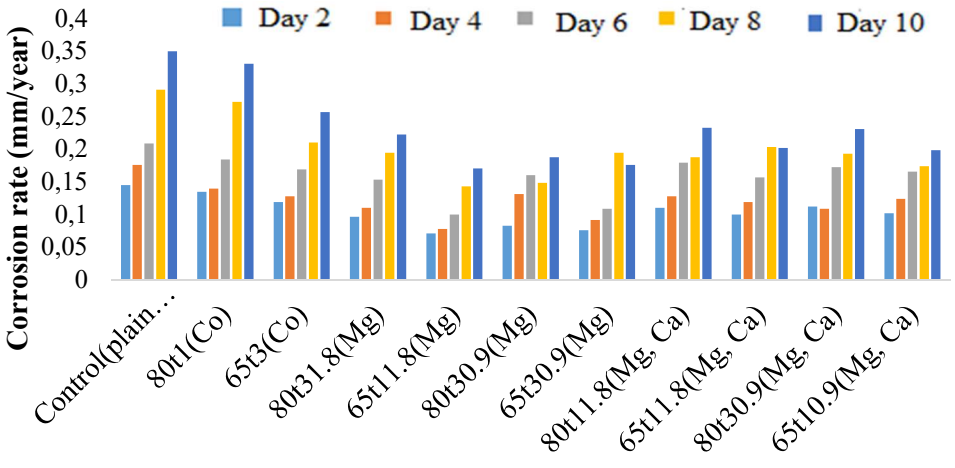

Figure 4: CR of the coated and uncoated samples.

In general, CR increased with time for each category of the tested samples. Non-phosphated MS control samples suffered higher CR than that from all other categories. Also, the two uncoated specimens (80t1C0 and 65t3C0) went through high CR. These

results confirmed that the phosphating technique is useful as a reliable technique for CR reduction, since PC samples experienced minimal level of corrosion.
A keen observation of the results also indicated that Mg-coated samples had lower CR than that from the specimen with Mg + Ca additives. This further established the good coating performance of Mg additive, and the less effective synergetic behaviour of Ca + Mg additives in the phosphating process.

IE(%)
Fig. 5 shows IE(%) of coated MS samples (based on every 2 day evaluation), for 10 days.

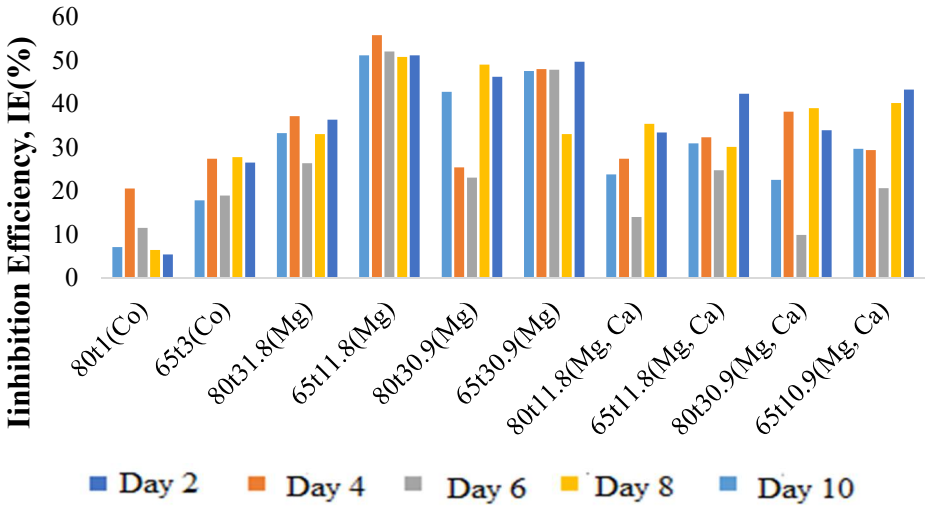

Figure 5: IE(%) of MS coated samples (with 2 day interval evaluation).

From the obtained results, it was seen that the samples coated at 65 ºC, with a Ct of 1.8 g/L Mg additive, at a phosphating time of 40 min, had the highest IE(%), followed by the specimens at 65 ºC, with a Ct of 0.9 g/L Mg additive, at phosphating time of 80 min. Plain unphosphated category had a very poor IE(%), lower than 20%.

Adsorption isotherm and thermodynamics properties
The results of Freundlich's plot of Mg and combined Mg and Ca additives adsorption for MS sample (at 65 and 80°C) are shown in Figs. 6 and 7, respectively.

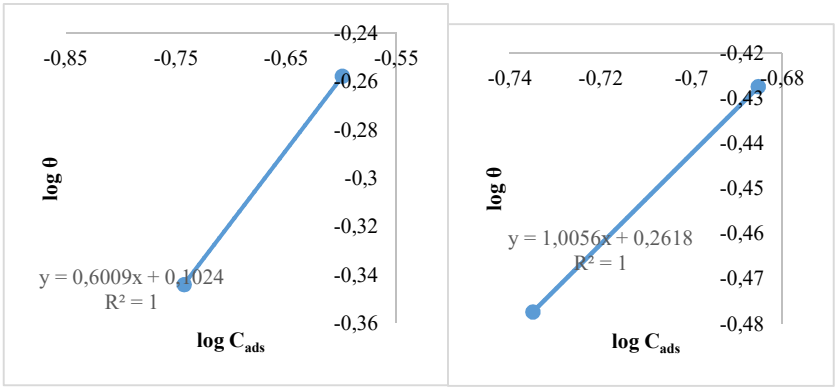

Figure 6: Freundlich's plot of Mg adsorption for MS sample at 65 (left) and 80 ºC (right).

The values of adsorption and thermodynamic parameters are listed in Tables 4 and 5. Good Mg and Ca adsorption was due to obtained K_{ads} positive values and ΔG_{ads} negative low values, in all cases. These values also indicated a physisorption process. Also, ΔH_{ads} negative values (in all cases) established the occurrence of heat loss to the environment during the coating process, while ΔS_{ads} negative values further revealed that it was not natural [17, 18].

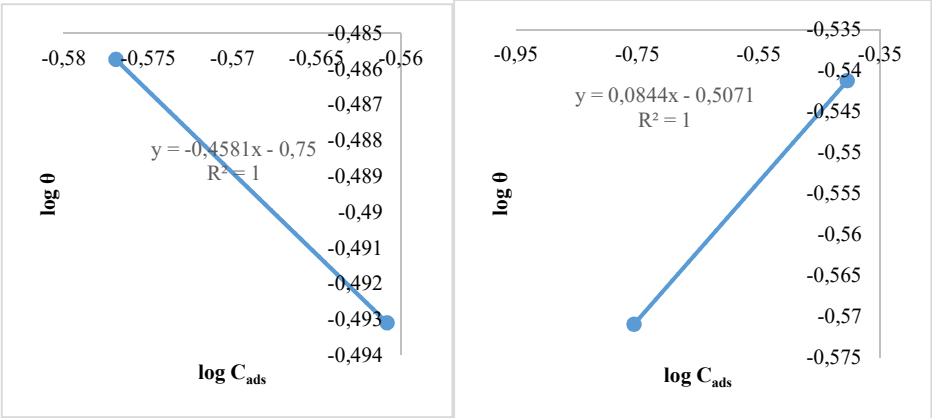

Figure 7: Freundlich's plot of Mg and Ca adsorption for MS sample at 65 (left) and 80 ℃ (right).

Table 4: Thermodynamic parameters derived from Freundlich's adsorption plot.

T (℃)	Additive	K_{ads}	ΔG_{ads} (J/mol)
65	Mg	1.2659	-11.9545
	Mg + Ca	0.1778	-6.4361
80	Mg	1.8273	-13.5624
	Mg +Ca	0.3111	-8.4571

Table 5: Thermodynamics property of PB with additives.

Additive	ΔH_{ads} (J/mol^{-1})	ΔS_{ads} ($J/mol^{-1}/K^{-1}$)
Mg	-71.406	-197.300
Mg + Ca	-37.0297	-95.145

Conclusion

The PB with 1.8 g/L Mg, at 65 °C, provided very reliable coating conditions with high corrosion resistance, in a 3.5 wt% NaCl solution.

SEM analysis and CR test for the coated MS showed that 65 °C was an optimum T for Mg-$Zn_3(PO_4)_2$ and even Mg-Ca-$Zn_3(PO_4)_2$, as it gave better results than those obtained at T of 80 °C. The greatest IE(%) of 55% was obtained for the MS sample, at 65 °C, with 1.8 g/L Mg. For 0.9 g/L Mg + 1.8 g/L Ca additives, an IE(%) of 32 was seen, at 65 °C. Mg and Mg/Ca additives adsorption onto the MS sample surface was well described by Freundlich's adsorption isotherm model. Calculated ΔG was negative, showing that the process was spontaneous and feasible. Negative ΔH showed that the reaction was exothermic. Negative ΔS during adsorption showed that the randomness degree decreased during the process.

Conflict of interest
The authors declare that there is no conflict of interest.

Authors' contributions
Ayoola A. A.: conception/design of the study, data acquisition, analysis and interpretation. **Durodola M. B., Babalola R., Fayomi O. S. I. and Okoji A.**: analysis and interpretation; critical revising. **Agbeyegbe G. A. and Obigwe C.**: design of the study; data acquisition, analysis and interpretation

Abbreviations
CR: corrosion rate
Ct: concentration
H_3PO_4: phosphoric acid
IE(%): inhibition efficiency
K_{ads}: adsorption rate constant
MS: mild steel
NaCl: sodium chloride
PB: phosphating bath
PC: phosphating coating
PO_4^{3-}: phosphate
SEM: scanning electron microscope
T: temperature
WL: weight loss
XRF: X-Ray fluorescence
$Zn_3(PO_4)_2$: zinc phosphate

Symbols definition
ΔG: change in Gibbs free energy
ΔH: change in enthalpy
ΔS: change in entropy

References
1. Loto RT. Comparative assessment of the synergistic combination of *Ricinus communis* and *Rosmarinus officinalis* on high-carbon and P4 low-carbon mold steel corrosions in dilute acid media. J Bio- Tribo-Corros. 2020;(4):47. https://doi.org/10.1007/s40735-018-0163-y
2. Zakeri A, Bahmani E, Aghdam ASR. Plant extracts as sustainable and green corrosion inhibitors for protection of ferrous metals in corrosive media: A mini review. Corros Comm. 2022;(5):25-38. https://doi.org/10.1016/j.corcom.2022.03.002
3. Juanbo L, Meng H, Sheng C et al. Corrosion inhibition effect of four inhibitors on SA106 Gr.B steel in coal-based syngas produced water. Int J Electrochem Sci. 2023;(18):100096. https://doi.org/10.1016/j/ijoes.2023.100096
4. Ayoola AA, Auta-Joshua N, Durodola BM et al. Combating A36 mild steel corrosion in 1 M H_2SO_4 medium using watermelon seed oil inhibitor. AIMS Mat Sci. 2021;(8):130. https://doi.org/10.3934/matersci.2021009

5. Ayoola AA, Fayomi OSI, Agboola O et al. Thermodynamics and adsorption influence on the corrosion inhibitive performance of pawpaw seed on A36 mild steel in 1 M H_2SO_4 medium. J Bio- Tribo-Corros. 2021;(7):128. https://doi.org/10.1007/s40735-021-00555-y
6. Loto RT. Surface coverage and corrosion inhibition effect of *Rosmarinus officinalis* and Zinc oxide on the electrochemical performance of low carbon steel in dilute acid solutions. Results Phys. 2018;(8):172-179. https://doi.org/10.1016/j.rinp.2017.12.003
7. Olayemi AO, Fayomi OSI, Tijani S et al. Chemical adsorption data, temperature effect and structural properties of artemether-lumefantrine corrosion inhibition properties on structural steel in 0.62 M NaCl. Key Eng Mat. 2021;886:281. https://doi.org/10.4028/www.scientific.net/KEM.886.143
8. Narayanan S. Surface pretreatment by phosphate conversion coatings – A review. Rev Adv Mat Sci. 2005;9:130-177.
9. Ezekiel SN, Ayoola AA, Durodola B et al. Data on zinc phosphating of mild steel and its behaviour. Chem Data Coll. 2022;(38):100838. https://doi.org/10.1016/j.cdc.2022.100838
10. Ayoola A, Ajinomisanghan E, Durodola B et al. Mild steel corrosion control through locally sourced calcium oxide on zinc phosphating process. South Afr J Chem Eng. 2023;(44):147-155. https://doi.org/10.1016/j.sajce.2023.02.001
11. Jegannathan S, Narayanan S, Ravichandran T et al. Formation of zinc–zinc phosphate composite coatings by cathodic electrochemical treatment. Surf Coat Technol. 2006;200(12-13):4117-4126. https://doi.org/10.1016/j.surfcoat.2005.04.022
12. Donofrio J. Zinc phosphating. Metal Finishing. 2010;108(11-12):40-56. https://doi. org/10.1016/s0026-0576(10)80212-0
13. Diaz BM, Freire M, Novoa, R. Optimization of conversion coatings based on zinc phosphate on high strength steels with enhanced barrier properties. J Electroanalyt Chem. 2014;737:174-183. https://doi.org/10.1016/j.jelechem.2014.06.035
14. Al-Swaidani AA. Modified zinc phosphate coatings: a promising approach to enhance the anti-corrosion properties of reinforcing steel. MOJ Civ Eng. 2017;3:5. https://doi.org/10.15406/mojce.2017.03.00083
15. Asadi V, Danaee I, Eskandari H. The effect of immersion time and immersion temperature on the corrosion behavior of zinc phosphate conversion coatings on carbon steel. Mater Res. 2015;18(4):706-713. https://doi.org/10.1590/1516-1439.343814
16. Ebelegi AN, Ayawei N, Wankasi D. Interpretation of adsorption thermodynamics and kinetics. Open J Phys Chem. 2020;10(03):166-182. https://doi.org/10.4236/ojpc.2020.103010
17. Popic J, Jegdic B, Bajat J et al. The effect of deposition temperature on the surface coverage and morphology of iron-phosphate coatings on low carbon steel. Appl Surf Sci. 2011;257(24):10855-10862. https://doi.org/10.1016/j.apsusc.2011.07.122
18. Banczek EP, Rodrigues PRP, Costa I. Investigation on the effect of benzotriazole on the phosphating of carbon steel. Surf Coat Technol. 2006;201:3701-3708.